Assessment of a Mining-Waste Dump of Galena Mine in the East of Morocco for Possible Use in Civil Engineering

Article *in* Journal of Ecological Engineering · February 2022

DOI: 10.12911/22998993/146585

7 authors, including:

El Khazanti Faical
Université Hassan 1er
2 PUBLICATIONS **1** CITATION

SEE PROFILE

JEE Journal of Ecological Engineering

Journal of Ecological Engineering 2022, 23(4), 336–349
https://doi.org/10.12911/22998993/146585
ISSN 2299–8993, License CC-BY 4.0

Received: 2022.01.20
Accepted: 2022.02.18
Published: 2022.03.03

Assessment of a Mining-Waste Dump of Galena Mine in the East of Morocco for Possible Use in Civil Engineering

Faiçal El Khazanti[1*], Ahmed Rachid[1], Achraf Harrou[2], Hicham Nasri[3], Yassine Ettayea[1], Meriam El Ouahabi[4], El Khadir Gharibi[2]

[1] Laboratory Physico-Chemistry of Processes and Materials (PCPM), Geology of Mining and Energy Resources (GRME), Faculty of Sciences and Technology, Hassan First University of Settat, 50 Rue Ibnou Lhaytham B.P. 577, 26002, Settat, Morocco

[2] Laboratory of Applied Chemistry and Environment, Mineral Solid Chemistry, Faculty of Sciences, Mohammed First University, Mohammed V avenue, Oujda 60000, Morocco

[3] Applied Geosciences Laboratory, Faculty of Sciences, University Mohammed First, Mohammed V avenue, Oujda, P.O. Box 60000, Morocco

[4] Laboratoire Argiles, Géochimie et Environnement sédimentaires (AGEs), Département de Géologie, Quartier Agora, Université de Liège, Bâtiment, B18, Allée du six Août, 14, Sart-Tilman, B-4000 Liège, Belgium

* Corresponding author's e-mail: f.elkhazanti@uhp.ac.ma

ABSTRACT

Mining dumps, particularly inactive or abandoned mines located near makeshift mining towns, have significant environmental and social impacts. The Touissit-Boubker lead mine, operated for years by the Touissit Mining Company (CMT) and abandoned without rehabilitation, is an example of this socio-economic and environmental collapse. Large quantities of harmful solid waste containing clayey aggregates rich in lead sulphide have been dumped in dykes on the edge of the village of Touissit. These mining wastes were rewashed to extract galena causing a depletion of lead sulphide. The objective of this study is to evaluate the possibility of using washed mining waste as sandy aggregate for the manufacture of masonry mortar. Cylindrical mortar tests, made with various proportions of sand and mine waste were characterized by X-ray diffraction, scanning electron microscopy and mechanical analysis by uni-axial compressive strength after curing for 3, 14, 28 and 60 days. The results obtained revealed that the mining waste consists of dolomite, quartz and clay. The dehydration rate of the mortar specimens is strongly affected by the amount of the waste added and the grain size. The mechanical strength of the mortar specimens mostly depends on the grain-size of the aggregates than on the amount of mine waste added. The microstructure of the mortar did not change when sand was replaced by mine waste of the same grain size.

Keywords: mining-waste; civil engineering; environment; masonry mortar; Touissit.

INTRODUCTION

World demand for certain minerals considerably increase since the end of the 19th century, which has led to the multiplication of mining projects, particularly concerning highly coveted metals, such as lead. Mining is vital to the world economy, but the extraction of metal compounds generates large quantities of waste (waste rock or slag) left in heaps, without any plant cover or development. This illegal action has led to divergent conflicts of interest between the operating companies and the local populations (Blaikie et al., 1995). The volume of waste produced is estimated to be in the thousands of millions of tons per year, and is increasing exponentially due to ever-increasing demand and the exploitation of low-grade deposits (Hudson-Edwards et al., 2015).

The Oriental region of Morocco has known an intense mining activity since the beginning of the 20th century. The most important are the iron mine of Ouksene, the lead mine of Touissit-Boubker,

the bentonite mines in Nador and the baryte mines in Nador and Figuig (ASM, 2015). The Touissit-Boubker Pb-Zn mining district is located close to the Algerian-Moroccan border, about 30 km south of the city of Oujda (Fig. 1A). Geologically, it is part of the Horsts chain, in the Missouine graben.

In Morocco, most of the mineralization hosted in sediment appeared much younger than suspected, and much younger than its host. The Touissit lead-zinc deposit hosted in the Jurassic limestone, settled in the Miocene (Fig. 1B) (Hudson-Edwards et al., 2015). The Touissit-Bou Beker district is the Mississippi Valley-type deposits, it is embedded in a thick sequence of dolomitized rocks by hydrothermal activities around 170 Ma, belonging to the Jurassic carbonate platform (Wadjinny, 1998, Bouabdellah, 2009, Marcoux et al., 2021). It comprises a Paleozoic basement consisting of metamorphites, granodiorites and rhyodacites and a tabular Mesocenozoic cover with calcareous Jurassic facies, a shallow calcarodolomitic layer of Aalenian-Bajocian age (Hauts Plateaux Slab), and by marly and detrital sediments of the Upper Jurassic (Fig. 1B).

The paragenesis of the lead mineralization consisted of more than 50–60% galena (PbS) with its oxidation products such as cerussite ($PbCO_3$), anglesite ($PbSO_4$) and wulfenite ($PbMoO_4$)), chalcopyrite (CuFeS) and rarely sphalerite. The gangue ore is mainly dolomite (Weiss, 1985). The clays present in the ore of Beddiane (Touissit) are kaolinite and illite (Bouabdellah, 2009).

The Touissit Mining Company operated the Touissit mine for 30 years (1974–2002). This mining activity has generated millions of tons of various types of waste in the form of mill tailings and waste rock (Fig. 2A).

The Touissit-Boubker polymetallic district produced 75 Mt of ores with 5% of Pb and 3% of Zn. This intense mining activity has been accompanied by the production of high amounts of liquid and solid mine waste (Rouleau, 2017). The solid wastes are stored in dikes on the outskirts of the village of Touissit (Bruneel, 2016). Indeed, the dykes of the Touissit mine contain traces of minerals leached by rainwater. They can have adverse effects on human health and the surrounding environment, in particular pollution of soil and water resources (Bell, 2001, Hakkou et al., 2008, Khalil et al., 2013).

The CMT washing plant used differential flotation to extract galena and blende. After the closure of the CMT, the site was abandoned, leaving ruins (workshops, washing plants), piles of mining waste rock and millions of tons of mining waste, stored in the slagheap. These have caused, under the influence of water and wind erosion, contamination of nearby water resources and soils (Rouleau et al., 2017). Other secondary activities were set up in the mining district to upgrade the waste by separating the ore from the gangue by washing. This activity has not solved the problem of waste accumulation, but it has greatly reduced their heavy metal content (Fig. 2B).

Several recent research have been conducted on mine wastes and their reuse in building materials (Pappu et al., 2007, Almeida et al., 2020) and in concreate (Ostrowski et al., 2020, El Machi et al., 2021). The building and civil engineering sectors, large consumers of raw materials, have shown great interest in recycling mine waste as alternative materials (Argane et al., 2016 Courard et al., 2019, Taha et al., 2018, Harrou et al., 2020, Oumnih et al., 2019). As the natural reserves of

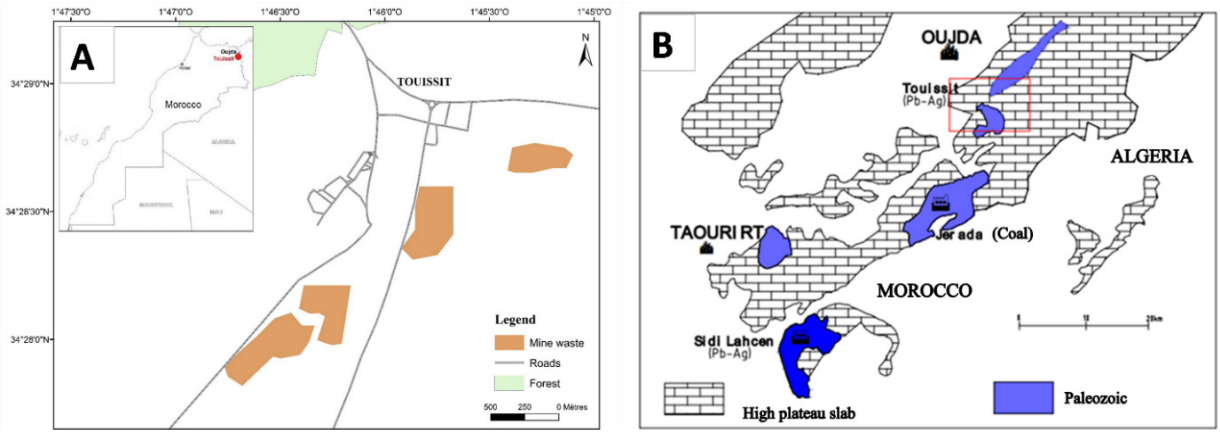

Figure 1. (A) Geographical situation of the Touissit mining dikes; (B) Geological context of the Touissit mine (Wadjinny, 1987)

Figure 2. Illustration of mining wastes from the Touissit mining district (A) washed mining waste of CMT, (B) rewashed mining waste from inclined-trough washing of OMC

sand are depleted due to high demand, there is a need to replace sand with waste rock and tailings in concrete (Gayana et al., 2018).

The abandoned mining wastes, from the Touissit-Boubker Pb-Zn mining district, contain significant quantities of Pb and Zn that inhibit setting and reduce mechanical strength of mortars (Argane et al., 2014).

The objective of this work is to study the impact of the washing in an inclined tank by Oriental Mining Company (OMC) of the mining waste of the CMT, on the mechanical strength and the reaction mechanisms in a masonry mortar made with sand-waste mixtures. The use of these wastes depleted from heavy metals by washing and rich in dolomite will have a positive economic and environmental impact.

MATERIALS AND METHODS

Raw material

The Oriental Mining Company operates the Touissit-Sidi Boubker mining wastes, abandoned by CMT. This company rewashed these rock wastes by gravitational washing to separate the recoverable galena. The rewashed waste, in the form of granulate low in lead sulphide, is stored in a slagheap.

Samples of rewashed waste, from OMC, were taken from the piles at different depths. They were dried, homogenized and sieved into different classes before their physical, chemical and mineralogical properties were determined.

Quarry calcareous sand from dolomitic quarry situated nearby the region was chosen as reference to manufacture mortar specimens.

CEN standard sand was used as a reference for grain-size distribution of quarry sand and mining waste.

The Portland cement for masonry CM 25, in accordance with the Moroccan standard NM 10.1.004, was used to manufacture the specimens.

Preparation of the specimens

The aggregates, waste and quarry sand, used in the mixtures are classified into four categories based on their grain size. The volume of water/cement and aggregate/cement ratios are 50 and 300 respectively.

The sand sampled from the quarry was sieved through four meshes: S1, S2, S3 and S4.

The mining waste rewashed were classified on four classes (W1, W2, W3 and W4) depending on their grain-size (Table 1). Class W0 corresponds to washed CMT waste, which has not been rewashed by Oriental Mining Company.

Table 1. Gain-size classes and the amounts of sand and waste used to manufacture mortars

Rewashed waste classes	Sand classes	Diameter	Ratio W/(S+W) (%)
W1	S1	125 < ϕ < 250 µm	0, 10, 20, 40, 60, 80, 90 et 100
W2	S2	ϕ < 125 µm	0, 50, 100
W3	S3	250 µm < ϕ	0, 50, 100
W4	S4	ϕ < 2000 µm	0, 50, 100

The prepared mortars are then placed in cylindrical molds with dimensions of 1.6 cm in diameter and 3.2 cm in height. They were kept in a closed box at 20±2°C and at 95% of moisture content for a curing period of 3, 14, 28 and 60 days (Fig. 3).

Characterization techniques

The raw materials, mining waste rock and natural quarry sand, were dried before analysis to ensure a consistent moisture level for all samples. Several physico-chemical and geotechnical techniques have been used to characterize the raw material and waste based specimens cured at 3, 14, 28 and 60 days at the Faculty of Sciences of the University of Oujda.

Grain-size distribution was determined by dry sieving according to the NF 933-1 standard. The water absorption coefficient, true and bulk density were obtained using standard geotechnical equipment according to EN 1097-3 and EN 1097-6 respectively. The true density does not depend on the degree of compaction of the material, while the bulk density has different values depending on whether it is measured in the free or compacted state (Derakhshani et al., 2015).

Infrared analysis was obtained using a Fourier transform spectrometer (FT/IR-4700, JASCO), ATR (attenuated total reflectance) mode, equipped with a DLaTGS detector and Peltier temperature control. A 10Hz scan with a resolution of 0.4 cm^{-1} was acquired in a wavelength range of 400–4000 cm^{-1}.

Thermal analysis was performed by thermogravimetry (TGA) and differential scanning calorimetry (DSC) by heating the samples from 20 to 1000 °C at a uniform temperature rate of 10 °C/min.

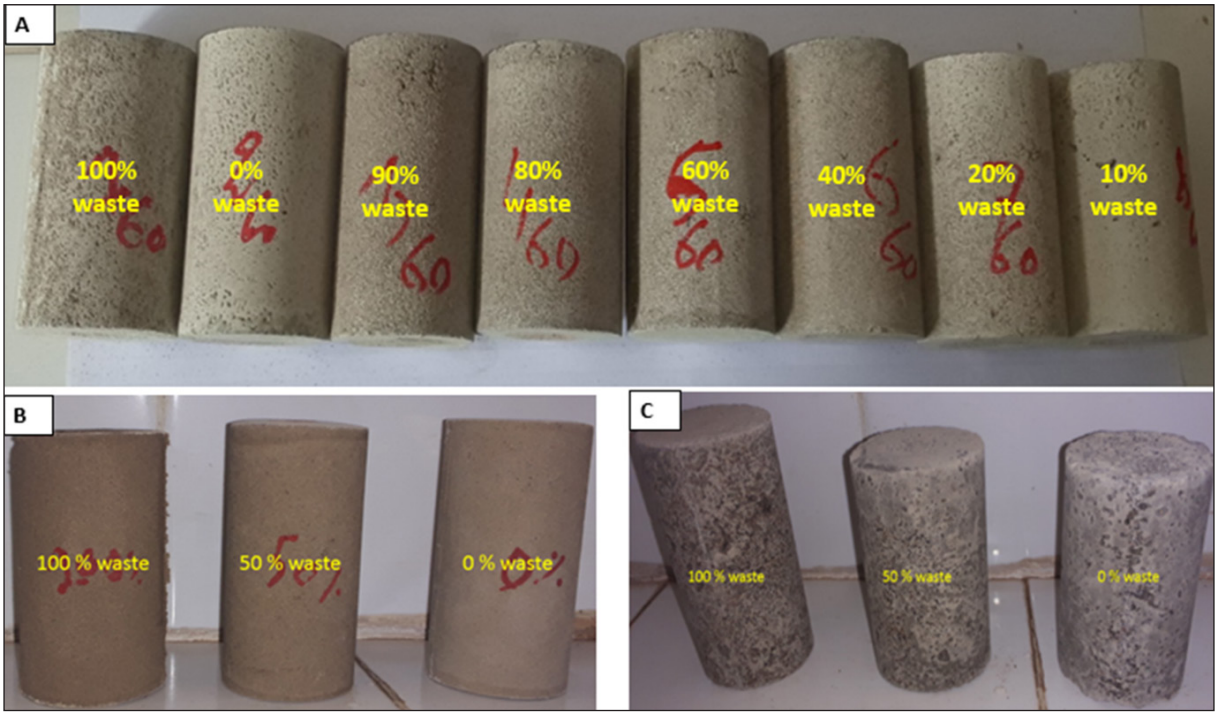

Figure 3. The appearance of prepared mortar specimens based on variable amounts of mining waste and quarry sand; (A) W1, S1 (125 <ϕ < 250 µm), (B) W2, S2 (ϕ < 125 µm) and (C) W3, S3 (250 µm < ϕ)

The TESTWELL apparatus with a speed of 0.5 mm/min allowed determining the compressive strength of the specimens.

At the Faculty of Science and Technology of Settat, Hassan I University, we have determined chemical and mineralogical compositions and microstructure. Chemical composition (XRF) was determined by X-ray fluorescence technique using PANalytical Epsilon 3X. X-ray diffraction (XRD) were performed on powder sample using the D2 PHASER diffractometer, equipped with a copper X-ray tube, operating at 40 kV and 30 mA, in the 2° – 70° 2θ range. Microstructure of the specimens was evaluated using a scanning electron microscopy SEM FEG JEOL JSM-IT500HR LV, equipped with Energy Dispersive X-Ray (EDX) detector.

RESULTS AND DISCUSSIONS

Characterization of raw materials

Physical properties

Figure 4 gives the grain-size distribution of mining waste, quarry sand and standard sand sample. The grain-size curves of quarry sand and mining waste show a continuous form, which will have a positive effect on the possibility of mixing them together, despite the high percentage of fine grains in mining waste sample. For quarry sand, widely used in constructions in the Oujda region, the curve is almost similar to that of standard sand sample. While, mining waste curve has a different particle size distribution, it shows a high percentage of fine particles. The average particle size is 250 µm. The fraction smaller than 63 µm, found by (Argane et al. 2014) in the washed mining waste W0, was 27% by weight. Gravitational rewashing reduces the < 63 µm particles to only 6% in W4.

Geotechnical and physical characteristics of the raw material used are shown in Table 2. Comparison between the parameters of quarry sand and standard sand shows a slight difference that can be attributed to the presence of fine grains in quarry sand. In mining waste, which contains a high percentage of fine grains, the parameters are different. The adsorption coefficient decreases with increasing size of aggregates (Tegguer, 2012). The bulk density is inversely opposed to the compression coefficient (Reichert et al., 2018). The density of dolomite, calcite and quartz is 2.86, 2.7 and 2.65 respectively that of sphalerite and galena are respectively 4.1 and 7.5. The presence of traces of the ore extracted from the Touissit deposit certainly increased the density of the mining waste samples. The low value of the sand fineness modulus leads to a decrease in workability (Belferrag, 2016). In other words, small variations in fineness modulus values of aggregate can affect the maneuverability of mortars (Gonçalves et al., 2007). A low sand equivalent value indicates impure aggregates and the existence of fine clay grains (Stefanidou, 2016).

Mineralogical and chemical proprieties

X-ray spectra of washed mining waste (Fig. 5A) show the dominance of dolomite, the presence of quartz and traces of kaolinite. Mineralogical

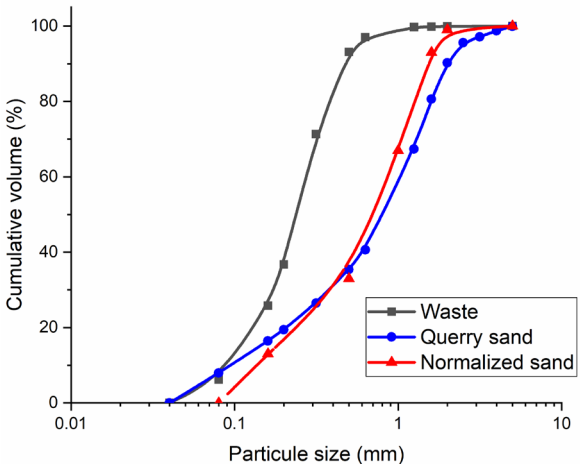

Figure 4. Particle size distribution of sand S4, standard sand and waste W4 (ϕ < 2000 µm)

Table 2. Physical parameters of sand S4 and mining waste W4

Physical properties	Sand	Waste	Standard sand
Apparent density (g/cm^3)	1.43	1.51	1.44
True density (g/cm^3)	2.65	2.82	2.54
Water absorption coefficient (%)	0.47	0.58	0.43
Fineness modulus	2.53	1.06	2.92
Sand equivalent (%)	84.81	71.6	100

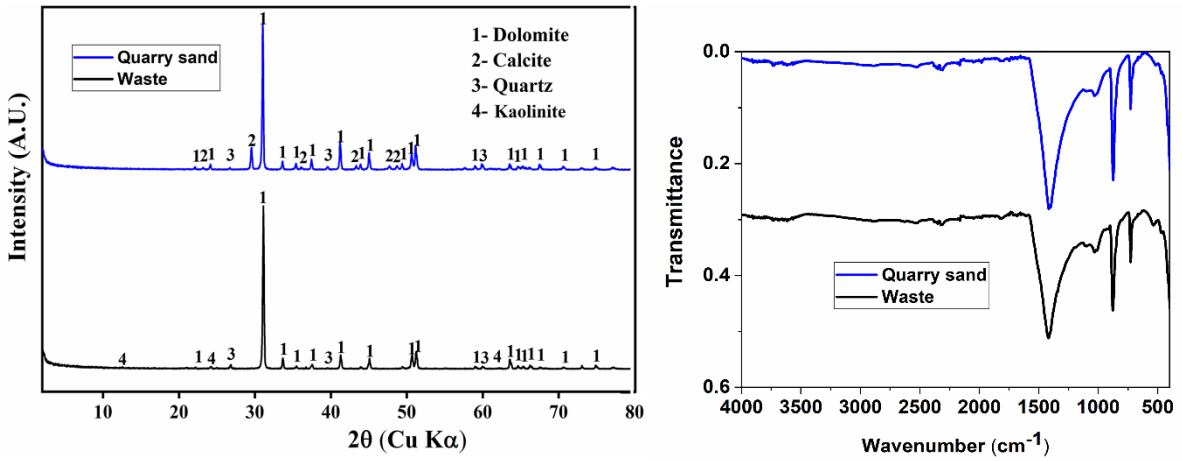

Figure 5. XRD and FTIR spectra of sand S4 and mining waste W4 (ϕ< 2000 µm)

composition of quarry sand consists of dolomite, quartz and calcite. Argane et al. en 2014 indicate the presence of silicates (quartz and orthose) and calcareous phases as dolomite, ankerite and smithsonite in raw mining waste.

FTIR spectrum of mining waste spectrum shows dolomite peaks observed at 1417 cm^{-1}, 877 cm^{-1} and 729 cm^{-1}, quartz peaks at 1100 cm^{-1}, 1030 cm^{-1} and 512 cm^{-1} (Fig. 5B). As for the quarry sand we observe the occurrence of three peaks 1396 cm^{-1}, 872 cm^{-1} and 713 cm^{-1} characteristic of vibration of CO_3^{2-} of calcite (Kim et al., 2021). The spectrum of quarry sand shows peaks at 1100 cm^{-1}, 1030 cm^{-1} and 538 cm^{-1} corresponding to quartz and dolomite.

Thermal proprieties

Thermogravimetry/Differential Thermal Analysis (TGA/DTA) of rewashed waste (W4) and finely grounded sand (S4) samples show similar trend with a slight shift towards high temperatures for waste sample (Fig. 6).

For waste, several endothermic peaks are observed in the DTA curve as the temperature increases. At low temperatures, an endothermic

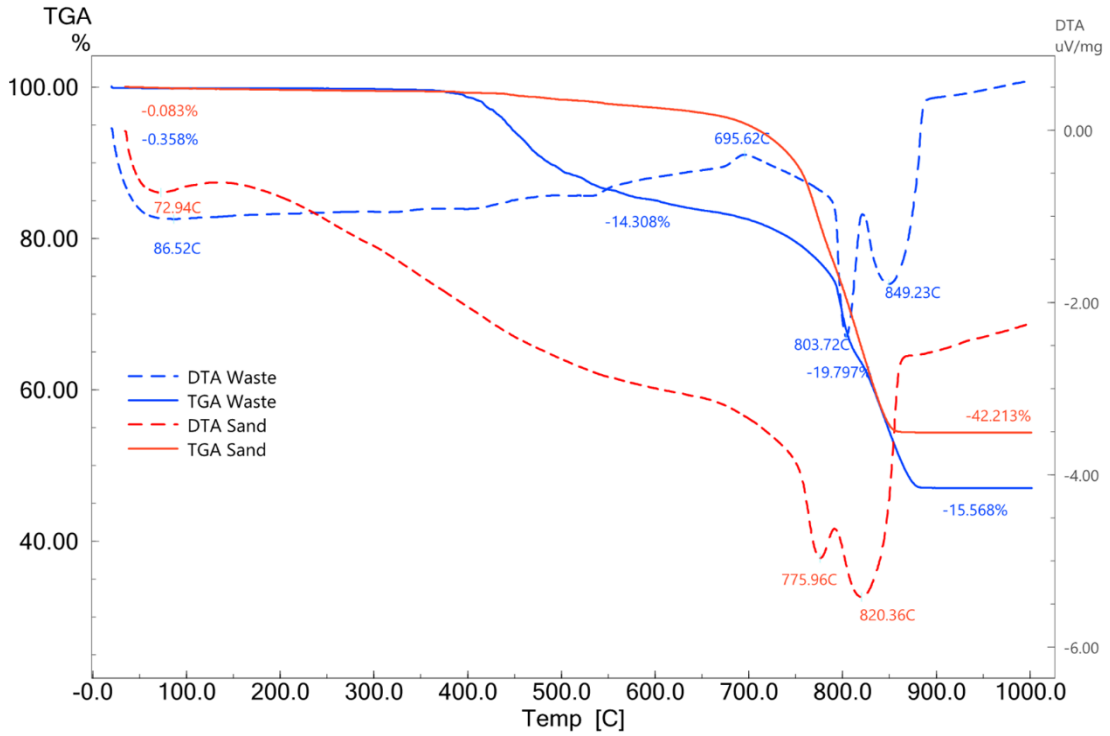

Figure 6. Thermogravimetry/Differential Thermal (TGA/DTA) spectra of mining waste W4 (ϕ < 2000 µm) and finely quarry sand S4 (ϕ < 2000 µm)

peak is observed due to the evaporation of zeolitic water. A large exothermic peak is also observed at 695.7 °C associated with a loss on weight of 14.1%, due to the decomposition of organic matter proliferated in waste stored for a long time on the surface (Delvigne, 1965). At high temperatures, the two peaks characteristic of dolomite decomposition appear associated with a loss of mass of 19.8% between 730 and 822 °C and 15.6% between 822 and 888 °C. The first is due to decomposition of dolomite to calcite and the second to decarbonation of calcite [Gunasekaran et al., 2007, Ratko et al., 2011, Olszak-Humienik et al., 2015). TGA curves show low mass losses at low temperatures corresponding to the evaporation of free water. The DTG confirms the double decomposition of dolomite according to the following equations:

$$CaMg(CO_3)_2 \rightarrow CaCO_3 + MgO + CO_2 ; \quad \Delta H_{20} = 124.6 \text{ kJ/mol} \quad (1)$$

$$CaCO_3 \rightarrow CaO + CO_2 ; \Delta H_{20} = 172.2 \text{ kJ/mol} \quad (2)$$

It is noted that temperatures of decomposition of dolomite and calcite in sand are lower than those of waste sample. Decomposition of organic matter followed by an increase in CO_2 partial pressure would result in the increase of decarbonation temperature of dolomite and calcite (Valverdeet al., 2015) In the quarry sand, the peak corresponding to the decomposition of calcite is more intense than that of dolomite.

Characterization of mortar specimens

Mortar dehydration rate

Figure 7 shows the dehydration rate of the mortar specimens as a function of time, obtained by weighing the mass of the specimens from the first day until the twenty-eighth day of maturation. The mass loss of mortar specimens made from fractions higher than 250 µm (W3, $\phi > 250$ µm, Fig. 7B), from the fine fractions (W2, $\phi < 125$ µm, Fig. 7C) and those containing all fractions (W4, $\phi < 2000$ µm, Fig. 7A) decreases when mining waste substitute quarry sand. The rate of mixing water is constant for all specimens.

The rate of dehydration decreases as the grain size increases. The increasing in content of the mixing water due to the fine particles, does not participate to the hydration process. Particles smaller than 63 µm, rich in fine particles, represent 27% by weight of the sample and therefore

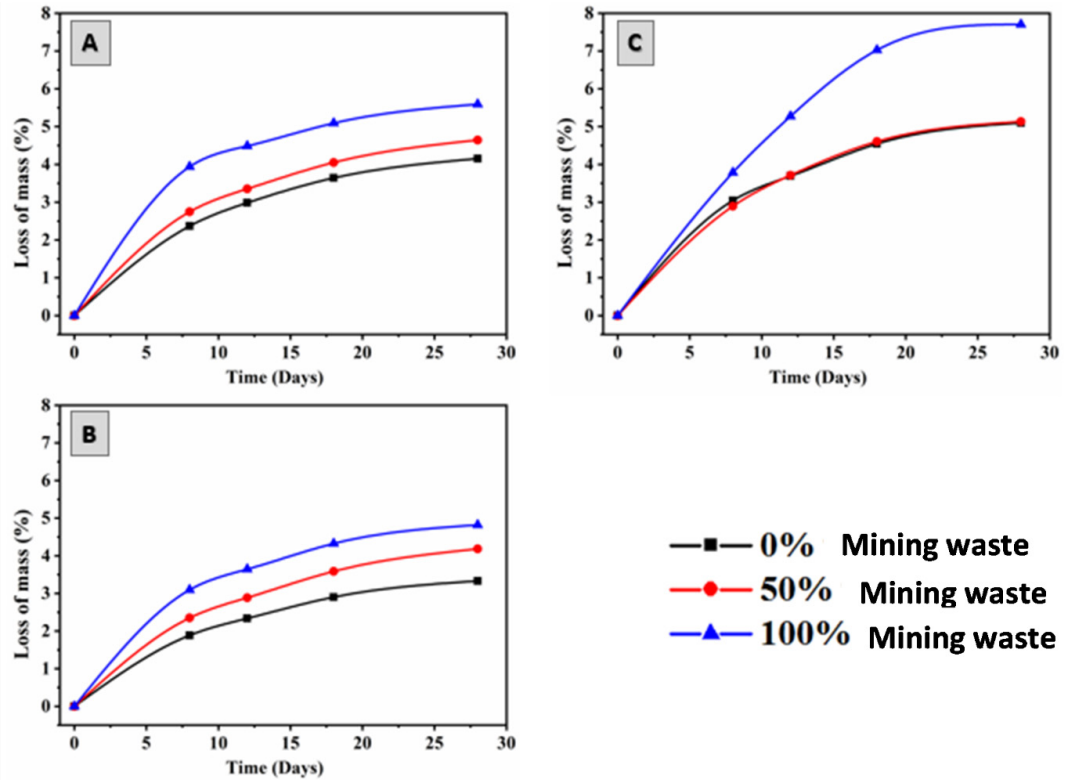

Figure 7. Loss on mass of specimens in terms of curing time.
(A) W4, S4 ($\phi < 2000$ µm), (B) W3, S3 ($\phi > 250$ µm), (C) W2, S2 ($\phi < 125$ µm)

require a large amount of water during mixing (Argane et al., 2014).

The mixing water is adsorbed by the clay fraction and evaporates by air during drying (Fig. 7C). For the three mixtures W2, W3 and W4, the rate of dehydration increases with the rate of replacement of sand by waste. Indeed, the amount of mixing water increases with the rate of sand replacement by waste (Wang et al., 2016).

Microstructure

The morphologies of the grains of the washed and the rewashed mining wastes are illustrated in Figure 8. Washed mining waste W0 shows a few fine grains (Fig. 8A) EDX spectrum reveals the occurrence of lead (Fig. 8B). SEM image of rewashed mining waste shows that rewashing removes fine particles (Fig. 8B). Lead is below the detection threshold in the rewashed waste (W4).

The semi-quantitative molar results, obtained by EDX, of the major elements in the two wastes W0 and W4 is given in Table 3. The gravitational rewashing has an effect on the concentrations of the major elements. The amount of magnesium dropped almost by half, while Ca remains stable.

X-ray fluorescence confirms the effect of rewashing on the mining waste, the amount of major metals in the Pb-Zn mine of Touissit-Boubker

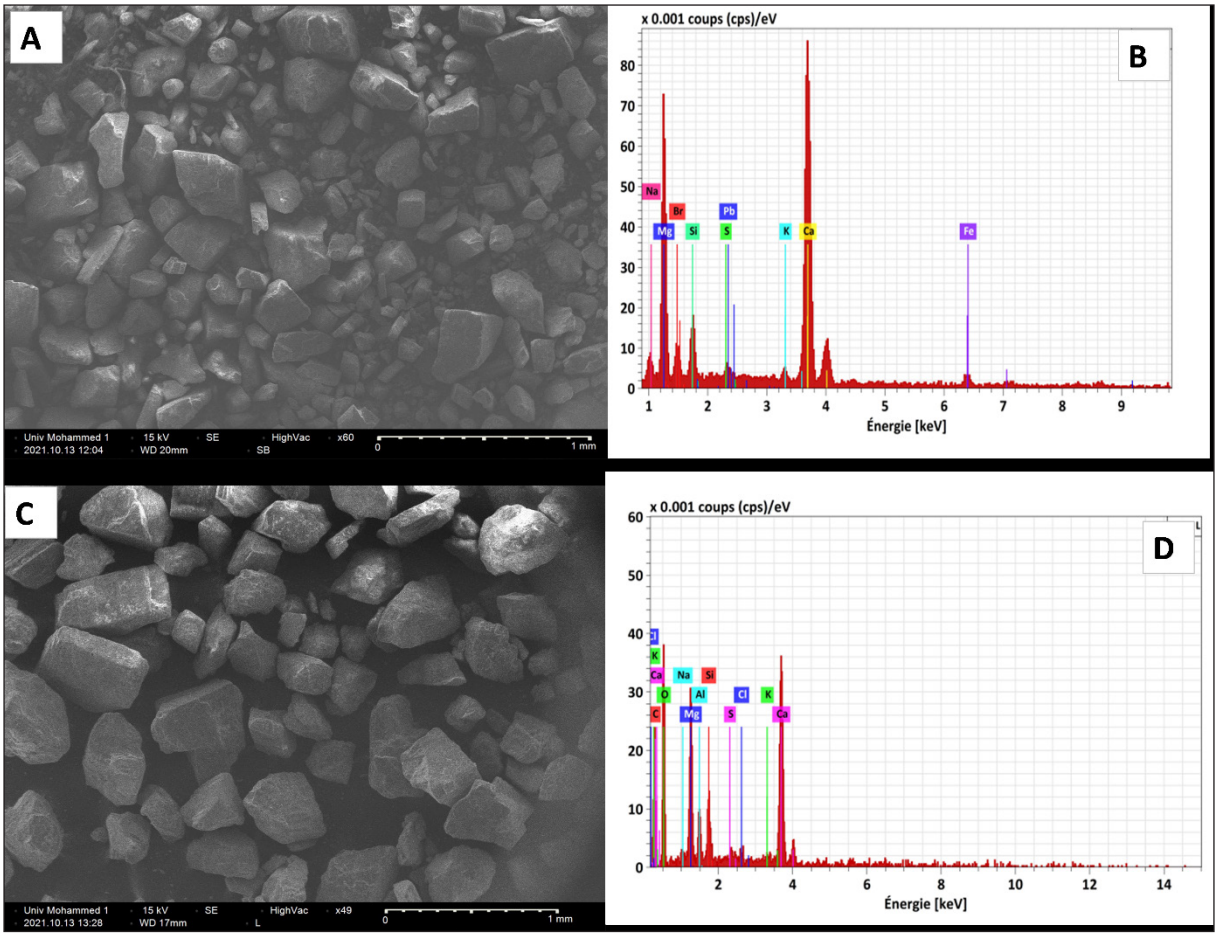

Figure 8. SEM images of (A) W0, CMT mining waste and (C) W4, OMC mining waste. EDX spectra of (B) W0, CMT washed mining waste and (D) W4, OMC rewashed mining waste ($\phi < 2000$ µm)

Table 3. EDX results of CMT washed waste W0 and OMC rewashed waste W4 ($\phi < 2000$ µm)

Element	CMT washed waste (W0) % atomic	Ratio/Ca	OMC rewashed waste (W4) % atomic	Ratio/Ca
Mg	6.19	1.15	3.58	0.76
Al	0.7	0.13	0.9	0.19
Si	0.77	0.14	1.01	0.21
Ca	5.36	1	4.71	1

Table 4. XRF results of CMT washed waste W0 and OMC rewashed waste W4 (ϕ < 2000 µm)

Mass (%)	MgO	Al_2O_3	SiO_2	K_2O	CaO	TiO_2	MnO	Fe_2O_3	CuO	ZnO	PbO	L.O.I.*
W0	10.46	3.52	8.02	0.28	30.54	0.20	0.30	3.08	0.22	1.87	1.40	47.6
W4	11.45	1.52	3.52	0.11	32.33	0.08	0.27	2.31	0.34	0.94	0.75	46.8
Mass (ppm)	SO_3	Cl	V_2O_5	SeO_2	SrO	SnO_2	HgO	Cr_2O_3	ZrO_2	Ag_2O	CdO	Sb_2O_3
W0	0	548.9	111.6	0	79.6	205.3	17.3	21.3	17.6	-	51.4	511.3
W4	212.5	489.8	57.5	-	46.4	-	-	8.3	21.2	883	59.5	487.6

* L.O.I. – loss on ignition.

district. A decrease in SiO_2 and Al_2O_3, which are the main components of clay phases, is observed after rewashing (Table 4). As for trace elements, a decrease in the most abundant metallic elements is also observed.

The Touissit-Boubker is known for mining Pb, Zn and Ag. In addition, traces of silver were recorded in galena and blende ore concentrates by the CMT company (Smouni, et al., 2010). The rewashing process slightly increased the silver content in the residue.

The paragenesis of lead mineralization consists of, among others, PbS, CuFeS and $PbSO_4$ (Weiss, 1985). Rewashing by the OMC has slightly increased the content of sulphate and sulphide insoluble.

Mechanical compressive strength

The compressive strength of mortar specimens made from quarry sand is slightly higher than that of specimens made from waste. As grain size increases, the mechanical performance of mortar specimens increases.

For W1, from the first 3 days of setting, a progressive decrease in compressive strength is observed as a function of the rate of substitution of sand by mining waste. This decrease was also observed for the substitution of sand by iron ore waste (Zhao et al., 2014). Between 10 and 60 days of curing, the compressive strength of specimens containing between 0% and 100% of waste, increases remarkably compared to early curing of 3 days (Fig. 9). A minimum uniaxial strength is observed when 50% of the sand is replaced by mining waste.

For specimen W2 made from 100% of waste shows no mechanical strength enhancement at any curing ages. On the other hand, the specimens made by 50% of waste show moderate compressive strength. In addition, the compressive strength of the specimens made by 50% of waste increased by 18.8%, 61.36% and 24.63% at 3, 14 and 28 days, respectively, compared to the mortar based on 100% of waste. The W3 samples show a progressive increase in strength from the first days of curing. W4 mortar, containing 50% of waste (Fig. 10) shows higher mechanical resistance than that of the reference mortars.

The decrease in strength observed on mortar specimens containing fine grains is firstly linked to the absorption of the mixing water. This decreases the W/C ratio and therefore the amount of water available for hydration that becomes insufficient when the water in the capillary pores is depleted. This lack of water then results in a slowing down of the hydration reaction at a young age (Powers, 1939). Indeed, increasing the content of fine fractions in mortar mixtures affects their workability, which may be dropped due to the increase in the total specific surface area of fine grains (Haach et al., 2011). Secondly, these fine mine waste grains contain heavy metals such as Pb and Zn. These metals are not removed during gravimetric separation and found in high content in the fine fractions < 32 µm (Khalil et al., 2019). The presence of these metals in an alkaline solution (pH = 13.11)

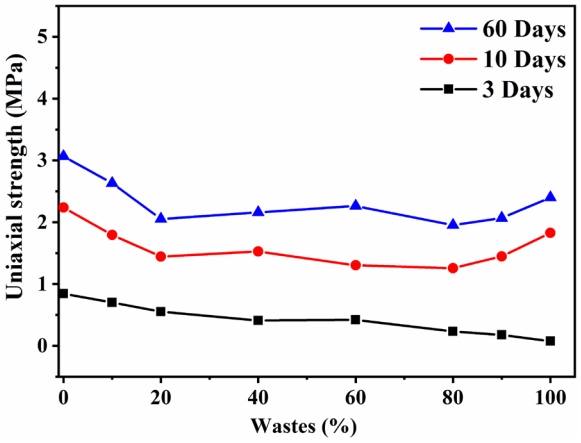

Fig. 9. Compressive strength of mortar specimens W1, S1 (125 < ϕ < 250 µm) at different percentage of waste cured for 3, 10 and 60 days

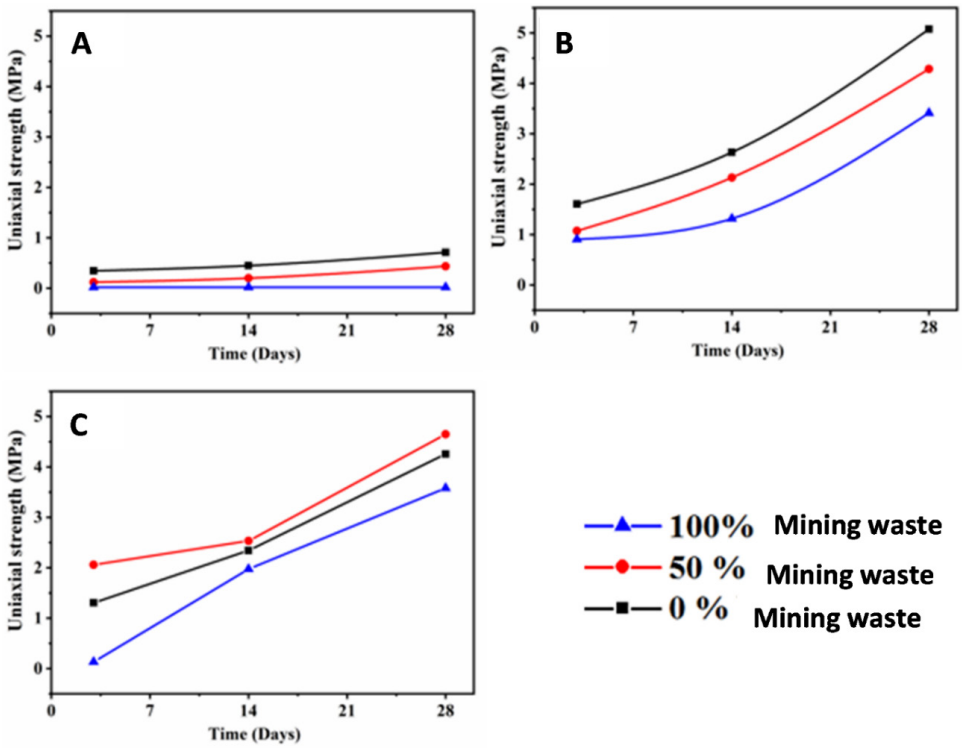

Figure. 10. Compressive strength evolution in terms of curing time of mortar specimens based on mixtures A: W2, S2 ($\phi < 125$ µm); B: W3, S3 ($\phi > 250$ µm) and C: W4, S4 ($\phi < 2000$ µm)

delays the setting of the mortar and prevents the formation of the main hydrated C-S-H and aluminate phases (McWhinney et al., 1990, Akhter et al., 1990), which confirms the absence of the C-H phase in the XRD results of W2 mortar.

The compressive strength values obtained in our study are almost similar to that of mortar stabilized iron ore tailing (Sun et al.,2011).

Mineralogical and microstructural characterization of mortars

The XRD results (Fig. 11) of the mortar specimens after 28 days of setting, show the formation of $Ca(OH)_2$ portlandite, which comes from the hydration of the calcium silicates of the Portland cement. In addition, the peaks of dolomite, calcite and quartz appear.

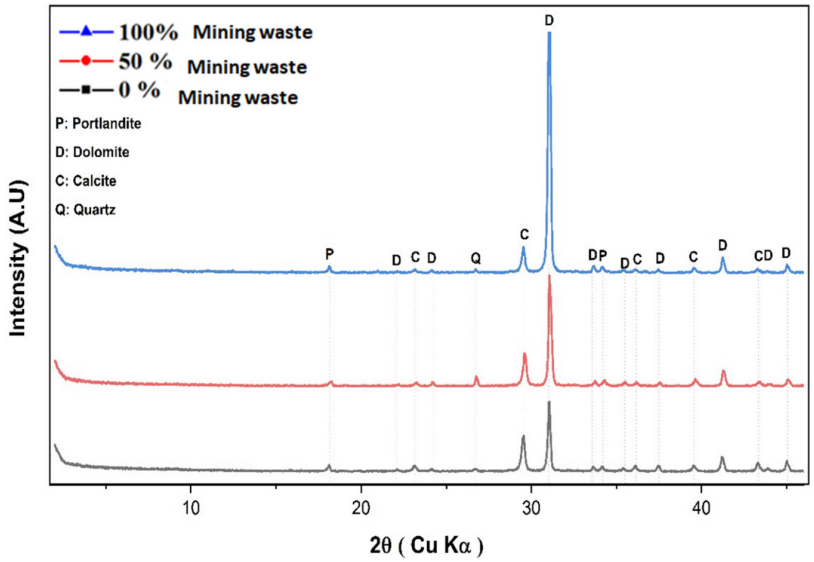

Figure 11. XRD spectra of cured mortar specimens of the mixtures W1, S1 ($125 < \phi < 250$ µm) for 0, 40 and 100% of mining waste added

SEM images (Fig. 12) show that the content of C-S-H, ettringite and portlandite of sample S1, containing only sand from the quarry, is higher than mortars containing mining waste (W1). Figure 12A shows a typical microstructure of a porous and homogeneous mortar (Yu et al., 2012). For a mortar made with fine mining waste (W2) (Fig. 12D), the development of the cement paste and the porosity is decreased due to the presence of fine particles in the waste. The clay particles block the hydration process of calcium silicates in Portland cement by adsorbing a large amount of the mix water. For particles with fine grains, the inter-particle voids are difficult to fill by the cement, which is the hydraulic link, and consequently the presence of air is trapped in the concrete, thus increasing its permeability (Perraton et al., 2001). Fine and very fine sands increase the macroporosity and reduce microporosity and cryptoporosity at high voltage (Dos Santos Souza et al., 2019).

The sample W1 shows an important development of the CH, C-S-H and portlandite phases, which enhances a cohesion between the grains (Fig. 12B). On the other hand, when waste is added to the cement without sieving (W4), low amounts of portlandite and C-S-H gel are formed. The gel formed is distributed between large grains of dolomite, which is the main component of mine waste studied (Fig. 12C).

CONCLUSIONS

The objective of this study is to meet both economic and environmental requirements: the substitution t of sand in concrete, because the depletion of natural sand reserves, by mine waste rock, and also the valorization of a large landfill of an inactive mine located near the city of Touissit.

Mining waste rock and natural quarry sand were physically, chemically and mineralogical characterized. Afterwards, cement specimens, manufactured with different proportions of sand and mining waste were manufactured and characterized. The uniaxial compressive strength of the specimens after curing of 3, 14, 28 and 60 days was evaluated.

The gravitational rewashing of the dolomite-rich Pb-Zn district mine waste, by reducing the content of metal sulphides and the rate of fine particles, makes mining waste suitable for replacing the natural sand from crushing quarries in masonry mortar.

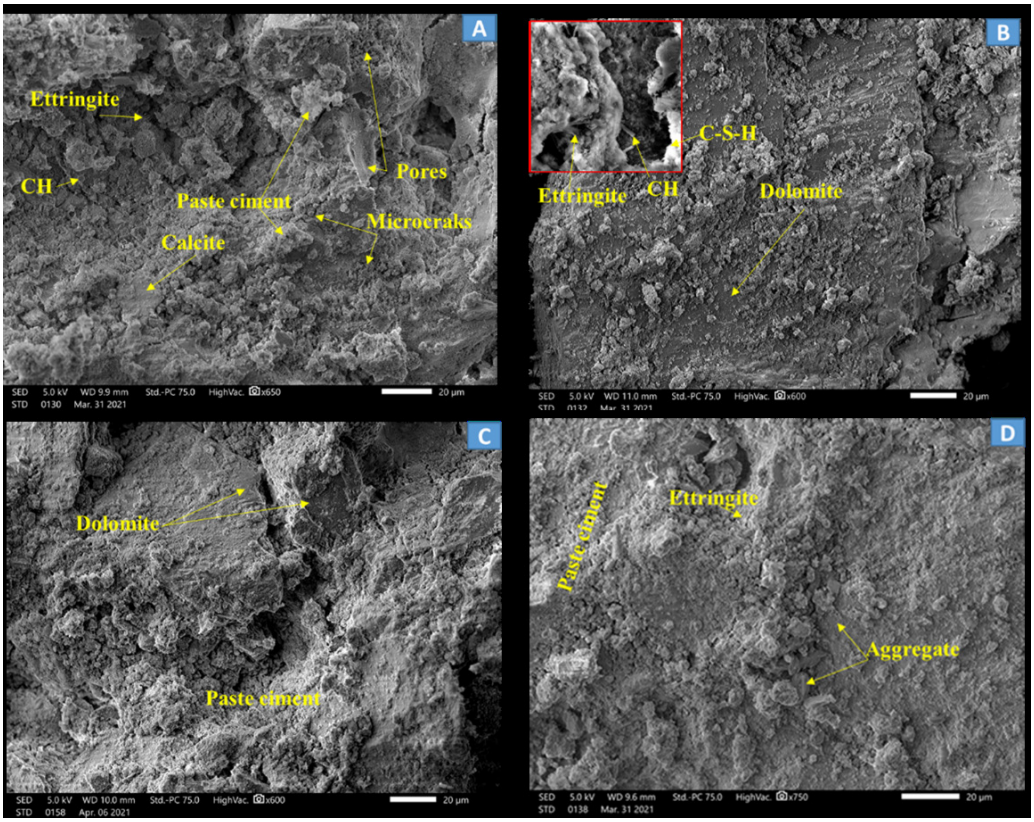

Figure 12. SEM images of mortar specimens. A: Quarry sand S1 ($125 < \phi < 250$ µm); B: mining waste W1 ($125 < \phi < 250$ µm); C: mining waste W4 ($\phi < 2000$ µm); D: mining waste W2 ($\phi < 125$ µm)

Mineralogical composition of waste and quarry sand are almost similar, consisting of dolomite. The rate of dehydration increases with the rate of replacement of quarry sand by mining waste and with the size of the grains of aggregates used.

Acknowledgements

The authors thank the manager of Oriental Mining Company for giving us samples of mining wastes and the department of chemistry of the faculty of sciences of Oujda for having allowed to realize the various analyses.

REFERENCES

1. Akhter H., Butler L.G., Branz S., Cartledge F.K., Tittlebaum M.E. 1990. Immobilization of As, Cd, Cr and Pb-containing soils by using cement or pozzolanic fixing agents. Journal of hazardous materials, 24(2-3), 145-155. https://doi.org/10.1016/0304-3894(90)87006-4
2. Almeida J., Ribeiro A.B., Silva A.S., Faria P. 2020. Overview of mining residues incorporation in construction materials and barriers for full-scale application. Journal of Building Engineering, 29, 101215. https://doi.org/10.1016/j.jobe.2020.101215
3. Argane R., Benzaazoua M., Bouamrane A., Hakkou R. 2014. Valorisation des rejets miniers du district Pb-Zn de touissit-boubker (région orientale-Maroc). Déchets Sciences et Techniques, 66, 38-44. https://dx.doi.org/10.4267/dechets-sciences-techniques.629
4. Argane R., El Adnani M., Benzaazoua M., Bouzahzah H., Khalil A., Hakkou R., Taha Y. 2016. Geochemical behavior and environmental risks related to the use of abandoned base-metal tailings as construction material in the upper-Moulouya district, Morocco. Environmental Science and Pollution Research, 23(1), 598-611. https://doi.org/10.1007/s11356-015-5292-y
5. ASM. 2015. Direction de la Statistique, Haut-Commissariat du Plan, Maroc.
6. Belferrag A. 2016. Contribution à l'amélioration des propriétés mécaniques et rhéologiques des bétons de sable de dunes (Doctoral dissertation, Université Mohamed Khider-Biskra).
7. Bell L.C. 2001. Establishment of native ecosystems after mining Australian experience across diverse biogeographic zones. Ecological Engineering, 17(2-3), 179-186. https://doi.org/10.1016/S0925-8574(00)00157-9
8. Blaikie P. 1995. Changing environments or changing views? A political ecology for developing countries. Geography, 203-214.
9. Bouabdellah M. 2009. Les paléo-karsts hydrothermaux à remplissage de sulfures du district de Touissit-Bou Beker (Maroc nord oriental): origine (s) et implication (s). Collection EDYTEM. Cahiers de géographie, 9(1), 23-32.
10. Bruneel O. 2016. Implication des microorganismes dans les biotransformations et processus de transfert des métaux et métalloïdes dans les environnements contaminés par les mines, Habilitation à Diriger des Recherches (Doctoral dissertation, Université de Montpellier).
11. Courard L., Tabarelli E., Michel F., Delvoie S., Bouarroudj M.E., Colman C., Zhao Z. 2019. Optimizing performances of recycled aggregates for improving concrete properties. Proceedings SMSS 2019.
12. Delvigne J. 1965. Pédogenèse en zone tropicale: la formation des minéraux secondaires en milieu ferrallitique 13. IRD Editions.
13. Derakhshani S.M., Schott D.L., Lodewijks G. 2015. Micro–macro properties of quartz sand: experimental investigation and DEM simulation. Powder Technology 269, 127-138. https://doi.org/10.1016/j.powtec.2014.08.072
14. Dos Santos Souza C., Antunes M.L.P., Dalla Valentina L.V.O., Rangel E.C., da Cruz N.C. 2019. Use of waste foundry sand (WFS) to produce protective coatings on aluminum alloy by plasma electrolytic oxidation. Journal of Cleaner Production 222, 584-592. https://doi.org/10.1016/j.jclepro.2019.03.013
15. El Machi A., Mabroum S., Taha Y., Tagnit-Hamou A., Benzaazoua M., Hakkou R. 2021. Use of flint from phosphate mine waste rocks as an alternative aggregates for concrete. Construction and Building Materials, 271, 121886. https://doi.org/10.1016/j.conbuildmat.2020.121886
16. Gayana B.C., Ram Chandar K. 2018. Sustainable use of mine waste and tailings with suitable admixture as aggregates in concrete pavements-A review. Advances in Concrete Construction, 6(3), 221-243.
17. Gonçalves J.P., Tavares L.M., Toledo Filho R.D., Fairbairn E.M.R., Cunha E.R. 2007. Comparison of natural and manufactured fine aggregates in cement mortars. Cement and Concrete Research, 37(6), 924-932. https://doi.org/10.1016/j.cemconres.2007.03.009
18. Gunasekaran S., Anbalagan G. 2007. Thermal decomposition of natural dolomite. Bulletin of Materials Science, 30(4), 339-344. https://doi.org/10.1007/s12034-007-0056-z
19. Haach V.G., Vasconcelos G., Lourenço P.B. 2011. Influence of aggregates grading and water/cement ratio in workability and hardened properties of mortars. Construction and Building Materials, 25(6), 2980-2987. https://doi.org/10.1016/j.conbuildmat.2010.11.011

20. Hakkou R., Benzaazoua M., Bussiere B. 2008. Acid mine drainage at the abandoned Kettara mine (Morocco): 2. Mine waste geochemical behavior. Mine Water and the Environment, 27(3), 160-170. https://doi.org/10.1007/s10230-008-0035-7
21. Harrou A., Gharibi E.K., Taha Y., Fagel N., El Ouahabi M. 2020. Phosphogypsum and black steel slag as additives for ecological bentonite-based materials: Microstructure and characterization. Mineral, 10(12), 1067. https://doi.org/10.3390/min10121067
22. Hudson-Edwards K.A., Dold B. 2015. Mine Waste Characterization, Management and Remediation. Minerals, 5, 82-85. https://doi.org/10.3390/min5010082
23. Khalil A., Hanich L., Bannari A., Zouhri L., Pourret O., Hakkou R. 2013. Assessment of soil contamination around an abandoned mine in a semi-arid environment using geochemistry and geostatistics: pre-work of geochemical process modeling with numerical models. Journal of Geochemical Exploration, 125, 117-129. https://doi.org/10.1016/j.gexplo.2012.11.018
24. Khalil N.M., Algamal Y. 2019. Environmental and economical aspects of partial replacement of ordinary Portland cement with Saudi raw minerals. Silicon, 11(1), 241-255. https://doi.org/10.1007/s12633-018-9929-6
25. Kim Y., Caumon M.C., Barres O., Sall A., Cauzid J. 2021. Identification and composition of carbonate minerals of the calcite structure by Raman and infrared spectroscopies using portable devices. Spectrochimica Acta Part A: Molecular and Biomolecular Spectroscopy, 261, 119980. https://doi.org/10.1016/j.saa.2021.119980
26. Marcoux É., Jébrak M. 2021. Plombotectonique des gisements du Maroc. BSGF-Earth Sciences Bulletin, 192(1), 31. https://doi.org/10.1051/bsgf/2021019
27. McWhinney H.G., Cocke D.L., Balke K., Ortego J.D. 1990. An investigation of mercury solidification and stabilization in Portland cement using X-ray photoelectron spectroscopy and energy dispersive spectroscopy. Cement and concrete research, 20(1), 79-91. https://doi.org/10.1016/0008-8846(90)90119-I
28. Olszak-Humienik M., Jablonski M. 2015. Thermal behavior of natural dolomite. Journal of Thermal Analysis and Calorimetry, 119(3), 2239-2248. https://doi.org/10.1007/s10973-014-4301-6
29. Ostrowski K., Stefaniuk D., Sadowski Ł., Krzywiński K., Gicala M., Różańska M. 2020. Potential use of granite waste sourced from rock processing for the application as coarse aggregate in high-performance self-compacting concrete. Construction and Building Materials, 238, 117794. https://doi.org/10.1016/j.conbuildmat.2019.117794
30. Oumnih S., Bekkouch N., Gharibi E.K., Fagel N., Elhamouti K., El Ouahabi M. 2019. Phosphogypsum waste as additives to lime stabilization of bentonite. Sustainable Environment Research, 29(1), 1-10. https://doi.org/10.1186/s42834-019-0038-z
31. Pappu A., Saxena M., Asolekar S.R. 2007. Solid wastes generation in India and their recycling potential in building materials. Building and environment, 42(6), 2311-2320. https://doi.org/10.1016/j.buildenv.2006.04.015
32. Perraton D., Aitcin P.C. 2001. Permeability of cover concrete: can choice of aggregates turn out to be more determinant than the W/C ratio? Bulletin des Laboratoires des Ponts et Chaussées.
33. PNM Projet de Norme Marocaine 10.1.045. 2020. Institut Marocain de Normalisation (IMANOR), 86
34. Powers T.C. 1939.The bleeding of potland cement paste, mortar, and concrete. Journal Proceedings, 35(6), 465-480.
35. Ratko A.I., Ivanets A.I., Kulak A.I., Morozov E.A., Sakhar I.O. 2011. Thermal decomposition of natural dolomite. Inorganic Materials, 47(12), 1372-1377. https://doi.org/10.1134/S0020168511120156
36. Reichert J.M., Mentges M.I., Rodrigues M.F., Cavalli J.P., Awe G.O., Mentges L.R. 2018. Compressibility and elasticity of subtropical no-till soils varying in granulometry organic matter, bulk density and moisture. Catena, 165, 345-357. https://doi.org/10.1016/j.catena.2018.02.014
37. Rouleau A., Gasquet D. 2017. Défis de la formation dans le secteur minier en Afrique francophone. L'industrie minière et le développement durable, 69. Institut de la Francophonie pour le développement durable (IFDD), Université du Québec à Chicoutimi, 133.
38. Smouni A., Ater M., Auguy F., Laplaze L., El Mzibri M., Berhada F. Doumas P. 2010. Évaluation de la contamination par les éléments-traces métalliques dans une zone minière du Maroc oriental. Cahiers Agricultures, 19(4), 273-279. https://doi.org/10.1684/agr.2010.0413
39. Stefanidou M. 2016. Crushed and river-origin sands used as aggregates in repair mortars. Geosciences, 6(2), 23. https://doi.org/10.3390/geosciences6020023
40. Sun J.S., Dou Y.M., Chen Z.X., Yang C.F. 2011. Experimental study on the performances of cement stabilized iron ore tailing gravel in highway application. Applied Mechanics and Materials, 97, 425-428. https://doi.org/10.4028/www.scientific.net/AMM.97-98.425
41. Taha Y., Benzaazoua M., Edahbi M., Mansori M., Hakkou R. 2018. Leaching and geochemical behavior of fired bricks containing coal wastes. Journal of environmental management, 209, 227-235. https://doi.org/10.1016/j.jenvman.2017.12.060

42. Tegguer A.D. 2012. Determining the water absorption of recycled aggregates utilizing hydrostatic weighing approach. Construction and Building Materials, 27(1), 112-116. https://doi.org/10.1016/j.conbuildmat.2011.08.018
43. Valverde J.M., Perejon A., Medina S., Perez-Maqueda L.A. 2015. Thermal decomposition of dolomite under CO_2: insights from TGA and in situ XRD analysis. Physical Chemistry Chemical Physics, 17(44), 30162-30176. https://doi.org/10.1039/C5CP05596B
44. Wadjinny A. 1987. Le district plombo-zincifère de Touissit : présentation géologique et métallogénique – Bulletin de l'industrie minérale, Les techniques, 70.
45. Wadjinny A. 1998. Le plomb au Maroc: cas des districts de Touissit et de Jbel Aouam. Chronique de la recherche minière, 9(28), 531-532.
46. Wang C.L., Ni W., Zhang S.Q., Wang S., Gai G.S., Wang W.K. 2016. Preparation and properties of autoclaved aerated concrete using coal gangue and iron ore tailings. Construction and Building Materials, 104, 109-115. https://doi.org/10.1016/j.conbuildmat.2015.12.041
47. Weiss N.L. 1985. Society of Mining Engineers (New York). Society of Mining Engineers of the American Institute of Mining, Metallurgical, and Petroleum Engineers SME mineral processing handbook, 2, 100-111.
48. Yu B. 2012. Les caractéristiques mécaniques et la microstructure du béton des granulats recyclés a hautes performances (Doctoral dissertation, Université de Lorraine).
49. Zhao S., Fan J., Sun W. 2014. Utilization of iron ore tailings as fine aggregate in ultra-high performance concrete. Construction and Building Materials, 50, 540-548. https://doi.org/10.1016/j.conbuildmat.2013.10.019